International Journal of Fatigue 70 (2015) 503–509

Contents lists available at ScienceDirect

International Journal of Fatigue

journal homepage: www.elsevier.com/locate/ijfatigue

Technical note

Modified Kitagawa–Takahashi diagram accounting for finite notch depths

J. Maierhofer [a,b,*], H.-P. Gänser [a], R. Pippan [b]

[a] Materials Center Leoben Forschung GmbH, Roseggerstraße 12, A-8700 Leoben, Austria
[b] Erich Schmid Institute of Materials Science and Department of Materials Physics University Leoben, Jahnstraße 12, A-8700 Leoben, Austria

ARTICLE INFO

Article history:
Received 24 April 2014
Received in revised form 21 July 2014
Accepted 24 July 2014
Available online 2 August 2014

Keywords:
Kitagawa–Takahashi diagram
Damage tolerance
Crack closure
Short cracks
Notch effects

ABSTRACT

The Kitagawa–Takahashi diagram in its commonly used form allows to predict, for cracks of given length and stress range, the allowable stress range for infinite life. However, caution is advised if a crack emanates not directly from the plane surface but from a sharp, crack-like notch instead. In this contribution, it is shown that taking the crack length equal to the total flaw depth (sum of notch depth and crack length) gives non-conservative results. Based on a simple mechanical model, a 3-dimensional Kitagawa–Takahashi diagram considering the build-up of crack growth resistance as well as the influence of the notch depth is developed. Comparison of model predictions and experimental results shows good agreement.

1. Introduction

The Kitagawa–Takahashi (KT) diagram [1] is a widespread tool for fracture mechanics based design of components and fracture control concepts such as the safe-life or fail-safe concepts. It combines the fatigue crack growth threshold and the fatigue endurance limit into a single plot, thereby defining the area of non-propagating cracks (leading to infinite fatigue life). Using the fictitious intrinsic crack length $a_{0,H}$ introduced by El Haddad [2], a smooth transition from the threshold of long cracks to the endurance limit is given (Fig. 1). This intrinsic length is computed as

$$a_{0,H} = \frac{1}{\pi}\left(\frac{\Delta K_{th,lc}}{Y \cdot \Delta\sigma_e}\right)^2 \quad (1)$$

and the endurance limit stress range dependent on the crack size a – i.e., the threshold stress range for crack propagation – is calculated by

$$\Delta\sigma_{th}(a_{0,H}) = \frac{\Delta K_{th,lc}}{Y \cdot \sqrt{\pi \cdot (a + a_{0,H})}}, \quad (2)$$

where $\Delta K_{th,lc}$ denotes the fatigue crack growth threshold for long cracks, $\Delta\sigma_e$ the endurance limit stress range of polished specimens without flaws, and Y is the geometry factor of the crack.

However, for cracks which have not built up crack closure completely (short cracks) the threshold of stress intensity range can be significantly smaller [3–7] and as a consequence the approximation according to El Haddad is non-conservative. So the build-up of crack closure has to be considered in the KT diagram. One method to describe the build-up of crack closure was proposed by McEvily and Minakawa [8], using an exponential function. Chapetti [9] used this exponential function to calculate the threshold stress for physically short cracks and showed that the threshold stress prediction obtained using the El Haddad correction is partially significantly higher, and therefore non-conservative. Similar behaviour has been shown by Tabernig et al. [10]. In other words, the endurance limit stress for physically short cracks is smaller than that one predicted using the intrinsic length scale $a_{0,H}$ according to El Haddad (see Fig. 1).

However, whereas Chapetti's approach to the KT diagram accounts for short crack effects, it still neglects the influence of the depth of a pre-existing flaw (which may be conveniently regarded as a sharp notch). In order to avoid non-conservative predictions, especially in the context of fracture control concepts, it is indispensable to account for effects due to the initial flaw. Tanaka and Akiniwa [4] investigated experimentally the influence of notch depth on the KT diagram and showed that the region of non-propagating cracks becomes smaller with increasing initial notch depth.

* Corresponding author at: Materials Center Leoben Forschung GmbH, Roseggerstraße 12, A-8700 Leoben, Austria.
E-mail addresses: juergen.maierhofer@mcl.at (J. Maierhofer), hans-peter.gaenser@mcl.at (H.-P. Gänser), reinhard.pippan@oeaw.ac.at (R. Pippan).

http://dx.doi.org/10.1016/j.ijfatigue.2014.07.007
0142-1123/

Nomenclature

Δa	crack extension length
a_0	notch depth
$a_{0,H}$	fictitious intrinsic length scale following El Haddad
a	total crack length
A	elongation at fracture
B	thickness of specimen
E	elastic modulus
H_V	Vickers hardness
ΔK	stress intensity factor range
ΔK_{th}	threshold of intensity factor range for crack propagation
$\Delta K_{th,eff}$	intrinsic (effective) threshold stress intensity factor range
$\Delta K_{th,lc}$	long crack growth threshold stress intensity factor range
l_i	fictitious length scales
L	length of specimen
R	load ratio
$R_{p0,2}$	0.2% offset yield stress
R_m	tensile strength
$\Delta\sigma$	stress range
$\Delta\sigma_e$	endurance limit stress range of polished specimens without flaws
$\Delta\sigma_{th}$	threshold stress range for crack propagation
$\Delta\sigma_{th,lc}$	threshold stress range for crack propagation calculated using $\Delta K_{th,lc}$
v_i	weighting factors
W	width of specimen
Y	geometry factor

In this paper, a modified KT diagram is developed that accounts for all of the aforementioned effects and is therefore readily applicable in the context of fracture control concepts in mechanical design.

2. Build-up of crack closure

The model for the build-up of crack closure at the threshold as proposed by the authors in [11] is based on a simple mechanical model as shown in Fig. 2.

To calculate the stress intensity factor

$$\Delta K = Y \cdot \Delta\sigma \cdot \sqrt{\pi \cdot a} \tag{3}$$

the total crack length

$$a = a_0 + \Delta a \tag{4}$$

is used, which is a combination of notch depth a_0 and crack extension Δa.

In contrast, for the build-up of crack closure not the total crack length a should be used, except the crack starts immediately at the surface of a component ($a_0 = 0$). If a crack starts from a notch (e.g., real design notches, casting defects or notches caused due to a forging lap, inappropriate handling, foreign object damage, et cetera) Δa must be used, because the crack flanks can be in contact only over this length. In other words, the notch depth a_0 is not subject to any crack closure even under compression loading; only by the crack extension Δa the build-up of crack closure is possible.

For the description of the threshold build-up starting from the intrinsic value of $\Delta K_{th,eff}$ at a crack extension of $\Delta a = 0$ to the long crack growth threshold $\Delta K_{th,lc}$ at large Δa, the empirical approach

$$\Delta K_{th} = \Delta K_{th,eff} + (\Delta K_{th,lc} - \Delta K_{th,eff}) \cdot \left[1 - \sum_{i=1}^{n} v_i \cdot \exp\left(-\frac{\Delta a}{l_i}\right)\right] \tag{5}$$

with the constraint

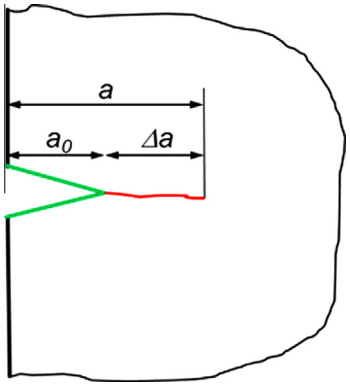

Fig. 2. Schematic illustration of the proposed mechanical model: emanating from a deep sharp notch a_0, a crack of extension Δa grows. Only on this crack extension Δa the build-up of crack closure is possible.

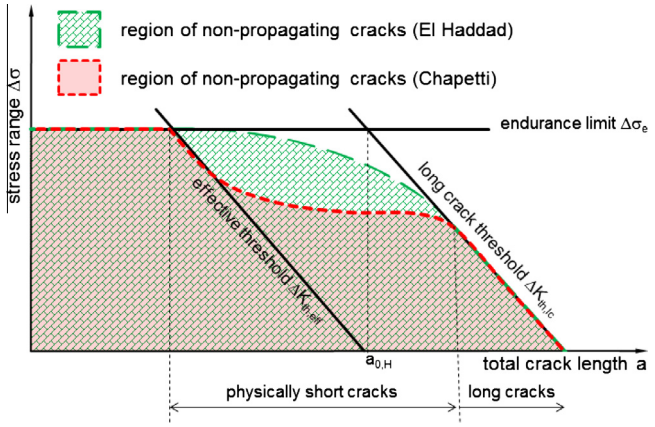

Fig. 1. Kitagawa–Takahashi diagram, showing the areas of non-propagating cracks according to El Haddad and Chapetti, respectively.

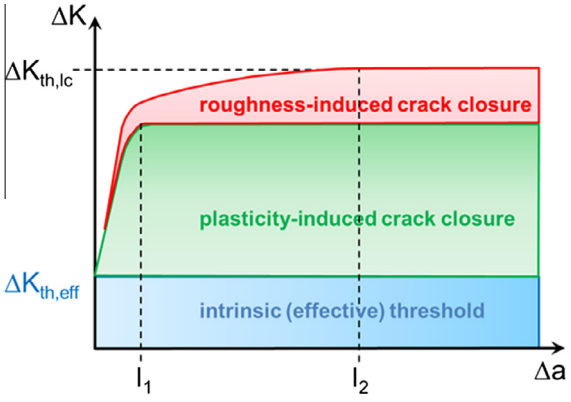

Fig. 3. Illustration of the crack resistance curve caused by two different closure mechanisms; each closure mechanism is built up completely over a specific crack extension (described by the fictitious length scales l_i).

$$\sum_{i=1}^{n} v_i = 1 \tag{6}$$

is used [11]. The l_i can be interpreted as fictitious length scales for the formation of crack closure effects (see Fig. 3), similar to El Haddad's $a_{0,H}$, and determined in conjunction with the v_i by fitting experimentally determined crack resistance curves (where ΔK_{th} is plotted against Δa). Such crack resistance curves may be obtained, e.g., from SENB (Single Edge Notched Bending) specimens with different notch depth, using the constant load increasing technique following the approach of Tabernig et al. [10]. The description of the increase of ΔK_{th} with crack length is in principle similar to the idea of McEvily and Minakawa [8]. However, the different l_i in this approach take into account that different crack closure mechanisms need different lengths to build up completely.

3. Considered example material

As material for the experimental investigations, the QT steel 25CrMo4 was chosen. The material has a bainitic microstructure without observable preferred orientation and a hardness of ~245 HV10. In the tensile test, a 0.2% offset yield stress of 512 MPa, a tensile strength of 674 MPa, and an elongation at fracture of 18.9% are obtained. The material properties are summarized in Table 1.

For determining the crack resistance curve (see Fig. 4) of the material, SENB specimens measuring $L = 100$ mm, $B = 6$ mm, $W = 20$ mm with different notch depths a_0 (0.35 mm, 1 mm, 5.3 mm) were machined. The notches were sharpened by means of razor blade polishing with diamond paste (1 μm). The samples were then compression pre-cracked at a load ratio of $R = 10$ to obtain a fatigue pre-crack. The samples are subjected to cyclic loading under eight-point bending in a resonance test rig at a testing frequency of 108 Hz. The crack growth is measured using the direct current potential drop (DCPD) method. The experiments are conducted under step-wise increasing constant loads. More detailed information about the experimental procedure to determine the crack resistance curve of this material can be found in [11]. The determined parameters for the model predictions are shown in Table 2.

4. Considering various notch depths in the KT diagram

The threshold stress range for crack propagation considering the model for build-up of crack closure introduced in Section 2 can now be calculated using Eqs. (3)–(5):

$$\Delta\sigma_{th} = \min\left(\frac{\Delta K_{th,eff} + (\Delta K_{th,lc} - \Delta K_{th,eff}) \cdot \left[1 - \sum_{i=1}^{n} v_i \cdot \exp\left(-\frac{\Delta}{l_i}\right)\right]}{Y \cdot \sqrt{\pi \cdot (a_0 + \Delta a)}}, \Delta\sigma_e\right), \tag{7}$$

where for very small total crack lengths the threshold stress range is limited by the fatigue endurance limit of polished specimens without flaws $\Delta\sigma_e$.

Table 1
Material properties for 25CrMo4.

Material property	Value	Unit
E	216	GPa
$R_{p0,2}$	512	MPa
R_m	674	MPa
A	18.9	%
H_V	245	HV10

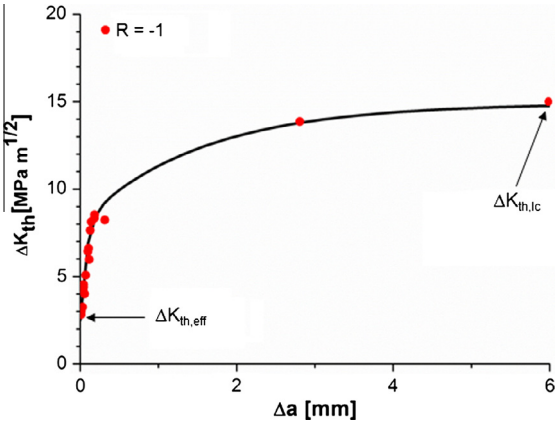

Fig. 4. Crack resistance curve: experimental data points and analytically estimation curve from Eq. (5).

Table 2
Parameters for the model predictions for 25CrMo4.

Parameter	Value	Unit
$\Delta K_{th,eff}$	2.5	MPa $m^{1/2}$
$\Delta K_{th,lc}$	14.65	MPa $m^{1/2}$
$a_{0,H}$	0.113	mm
l_1	0.08	mm
l_2	1.55	mm
v_1	0.45	–
v_2	0.55	–
Y	1.12	–

Using Eq. (7), the threshold stress range for any notch depth a_0 and crack extension Δa can now be determined. In Fig. 5a, a three-dimensional extension of the KT diagram is shown, varying both the notch depth a_0 and the crack extension Δa. In Fig. 5b, in addition the conventional threshold stress range

$$\Delta\sigma_{th,lc} = \frac{\Delta K_{th,lc}}{Y \cdot \sqrt{\pi \cdot (a_0 + \Delta a + a_{0,H})}} \tag{8}$$

calculated using El Haddad's approach, Eq. (2), is plotted (grey surface). It is assumed that a_0 and Δa are small compared to the component size, and that the stress gradients are small. A comparison between these surfaces shows that they are congruent for long crack extensions Δa (i.e. for cracks which have built up their crack closure completely). However, for short crack extensions a lifetime estimation based on El Haddad's approach can lead to non-conservative results, because crack propagation is possible also at stress ranges far below the limit given by Eq. (8) (and actually most likely, as Fig. 5b implies). To emphasize the difference between the conventional KT diagram and the new approach, cuts have been made through this 3-dimensional illustration of the KT diagram along the a_0 and Δa directions. Fig. 6 shows one at a constant notch depth ($a_0 = 1$ mm, curve 1) and another at a constant crack extension ($\Delta a = 1$ mm, curve 2). The lines 3 and 4 represent the respective intersections with the non-conservative threshold stress range according to Eq. (8). Here, the cuts were also done at constant notch depth or constant crack extension, respectively, of 1 mm.

A comparison of these curves shows clearly why it is useful to account separately for notch depth a_0 and crack extension Δa, and therefore to introduce an additional axis in the KT diagram. In Fig. 7a the cuts from Fig. 6 are compared. The total crack length $a = a_0 + \Delta a$ of all curves is identical for each point on their respective X-axis. However, curve 1 deals with a constant notch depth a_0 and increasing crack extension Δa, whereas curve 2 deals with constant crack extension and increasing notch depth. Curve 3 is,

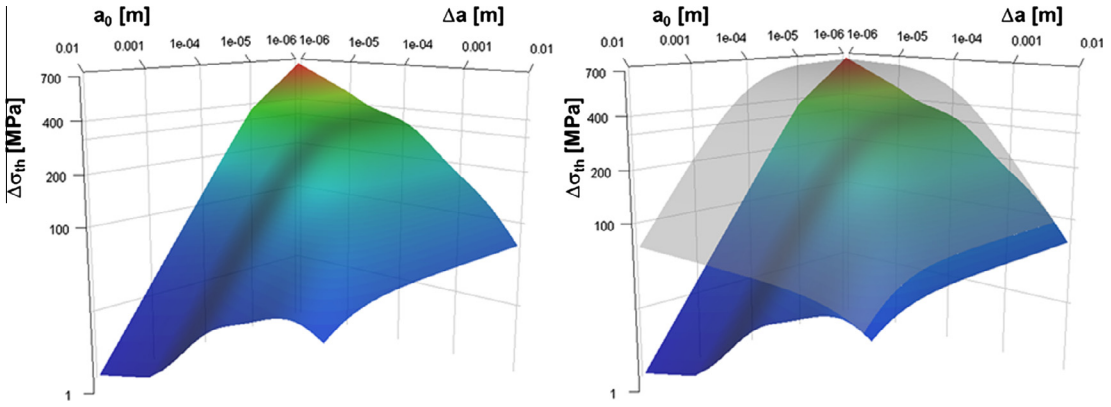

Fig. 5. Threshold stress range $\Delta\sigma_{th}$ plotted over crack extension Δa and notch depth a_0 (three-dimensional Kitagawa–Takahashi diagram).

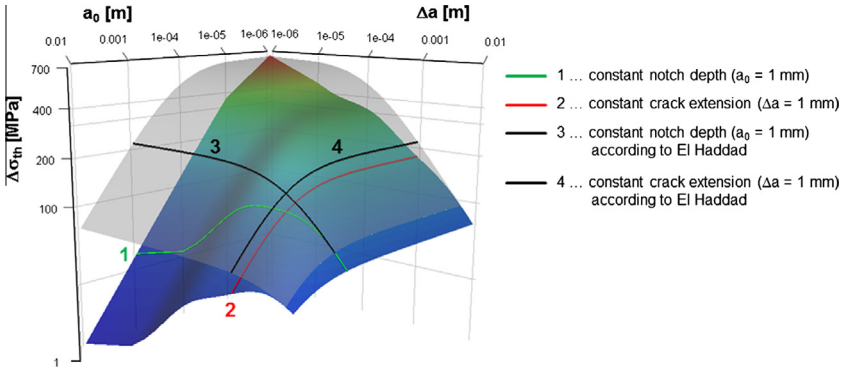

Fig. 6. Cuts in the 3-dimensional KT diagram at constant notch depth $a_0 = 1$ mm and at constant crack extension $\Delta a = 1$ mm, respectively.

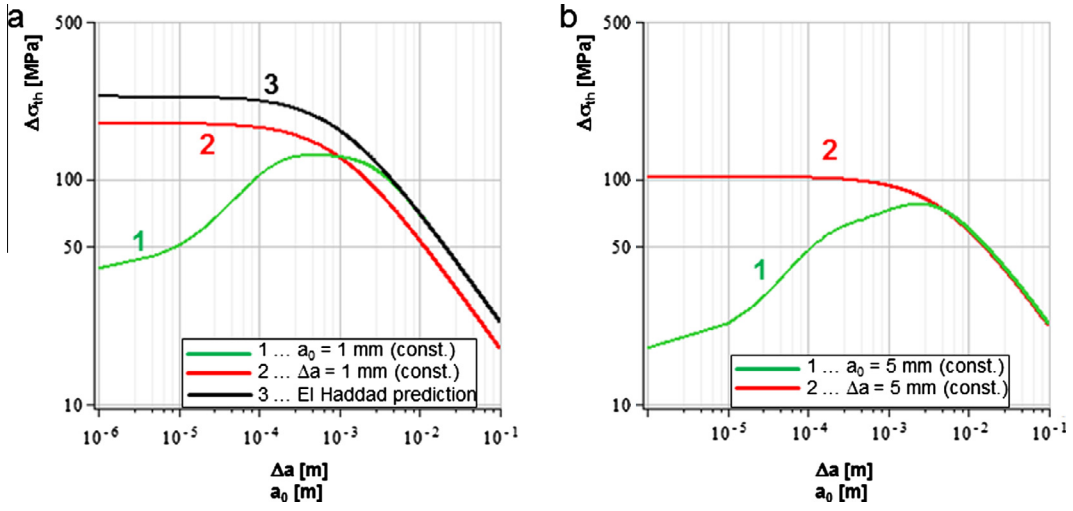

Fig. 7. Comparison of two cracks with the same total crack length a – the green line for a constant notch depth varying the crack extension and the red line with a constant crack extension varying the notch depth. The conventional prediction following El Haddad, Eq. (8), is shown in black. (For interpretation of the references to colour in this figure legend, the reader is referred to the web version of this article.)

due to the symmetry of Eq. (8), identical for increasing a_0 and increasing Δa.

The region of non-propagating cracks predicted from Eq. (7) for a constant notch depth (under curve 1) is now completely different to the region predicted from a constant crack extension (under curve 2), although the total crack length a is the same for each point of the X-axis. As the fatigue crack builds up crack closure only with increasing crack extension Δa, curve 1 starts at a low limit of stress ranges where no crack propagation occurs corresponding to the intrinsic crack growth threshold and increases gradually due to the build-up of closure until it reaches the long crack prediction given by the inclined branch of curve 3. Curve 2 for constant crack extension $\Delta a = 1$ mm lies somewhat below the conventional El Haddad prediction (Eq. (8), curve 3) as crack closure is not yet fully developed at $\Delta a = 1$ mm. In contrast, Fig. 7b shows the analogous curves for $a_0 = 5$ mm and $\Delta a = 5$ mm. Here, crack closure is fully

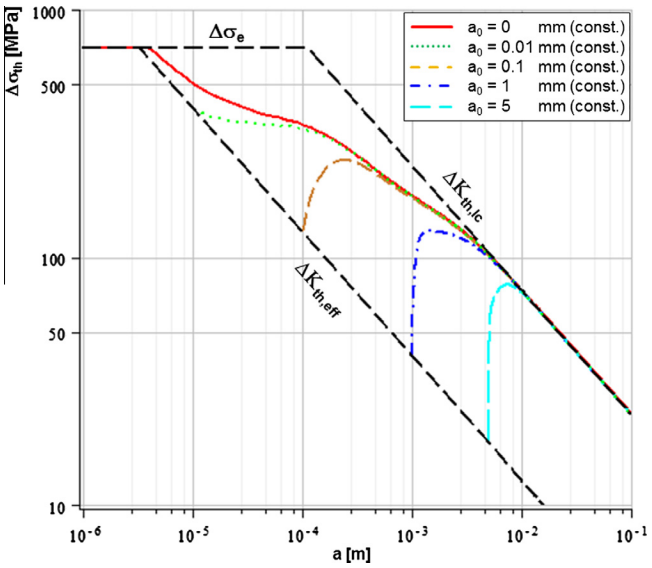

Fig. 8. Limiting curves for non-propagating cracks in dependence of notch depth a_0 and total crack length $a = a_0 + \Delta a$.

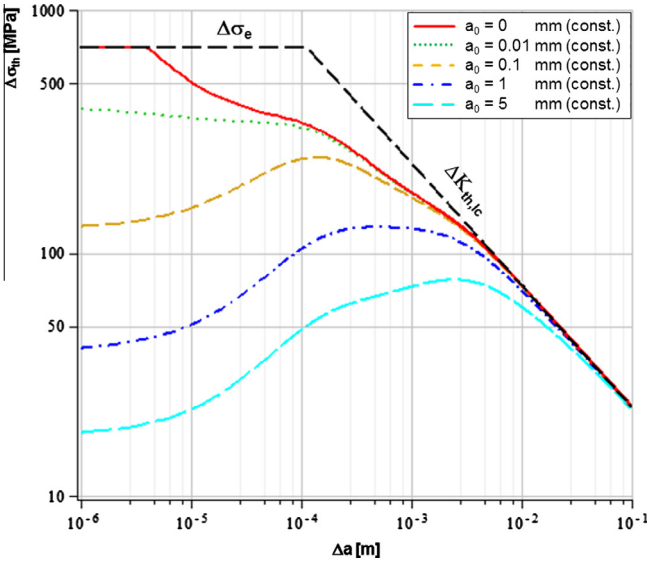

Fig. 9. Threshold stress range against crack extension emanating from different notch depths.

developed for curve 2, and so this curve is identical to the conventional El Haddad prediction. Curve 1 shows again the gradual build-up of crack closure until it approaches the long crack prediction.

If one plots the intrinsic threshold for crack propagation $\Delta K_{th,eff}$ and the long crack threshold for crack propagation $\Delta K_{th,lc}$ in a double logarithmic diagram against the total crack length $a = a_0 + \Delta a$, it is rather easy to estimate the limiting curves for non-propagating cracks. The threshold stress range $\Delta\sigma_{th}$ of non-propagating cracks of total length $a = a_0$, extension $\Delta a = 0$, and therefore non-existent closure, is given by:

$$\Delta\sigma_{th}(a = a_0) = \frac{\Delta K_{th,eff}}{Y \cdot \sqrt{\pi a_0}} \tag{9}$$

Now it depends on the length of the notch how steep the limiting curve is in the beginning. The deeper a notch, the steeper is the initial increase of the limiting curve. After a certain increase the limiting curve becomes shallower and finally approaches the asymptotic line given by the long crack threshold $\Delta K_{th,lc}$, see also Fig. 8. Here for different notch depths the associated limiting curve for non-propagating cracks are plotted over the total crack length a. The curves are limited by an upper bound due to the endurance limit.

In Fig. 9, the threshold stress range for various notch depths a_0 is plotted against the crack extension Δa only. One can see that, for shallow notches, crack closure is not built up sufficiently fast to generate cracks which stop after a certain crack extension. That means that the region of non-propagating cracks (the area below the threshold stress range) is much larger for cracks emanating from a shallow notch or from a smooth surface than for cracks emanating from deep notches. Moreover, from this figure one can easily extract the allowable crack extension for a given applied stress range. Supposed we have an applied stress range of 100 MPa and a notch of 1 mm depth. For these conditions the crack is able to grow until a crack extension of approximately 0.1 mm is reached. Then the crack will arrest, whereas for a notch of 5 mm depth an applied stress range of 100 MPa would lead to finite life (the corresponding curve for non-propagating cracks does not reach the value of 100 MPa).

To verify the model predictions, experiments with three different notch depths (0.813 mm, 2.19 mm and 5.39 mm) were performed. In Fig. 10 the theoretically possible crack extensions due to the predicted threshold stress curves are drawn as red dashed lines. The crack can grow until the crack extension Δa intersects the predicted threshold curve, where crack arrest occurs. Subsequently, the load may be increased until either crack arrest occurs

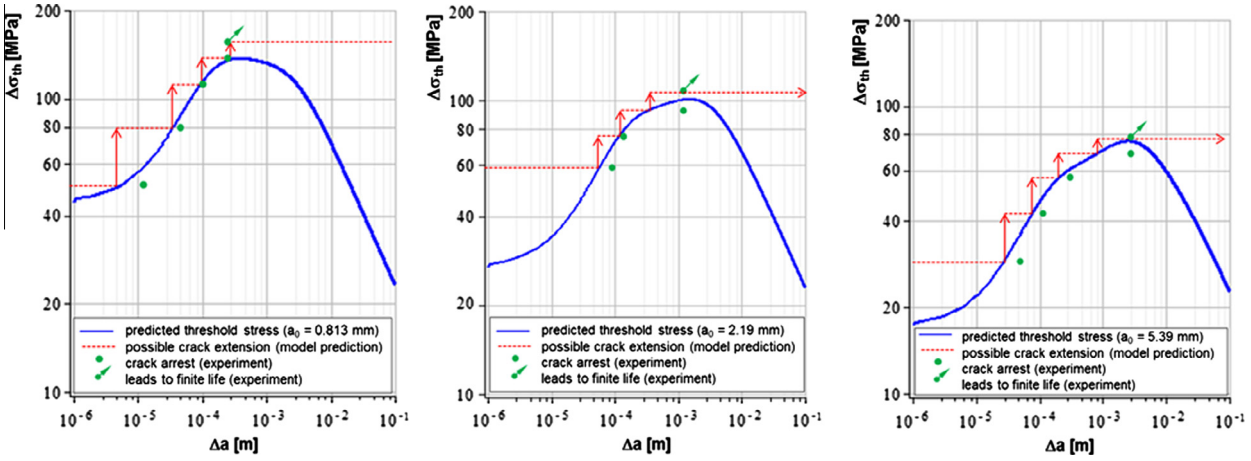

Fig. 10. Comparison of the crack extension predicted from the threshold stress range with experimental results for samples with different notch depths $a_0 = 0.81$, 2.19, 5.39 mm.

Table 3
Comparison between experimental and predicted threshold stress range.

Notch depth a_0 (mm)	Experimental determined Δa (mm)	Threshold stress range $\Delta\sigma_{th}$ (MPa)		Discrepancy (%)
		Experiment	Prediction	
0.813	0.011	51.2	57	10.2
	0.042	79	84.6	6.6
	0.1	112	113.6	1.4
	0.185	133.4	130.4	2.3
2.19	0.094	58	70.3	17.5
	0.135	74	78.5	5.7
	1.181	90.4	93.8	3.6
5.39	0.055	28.7	37.2	22.8
	0.114	42.7	51.8	17.6
	0.313	56.5	60.6	6.8
	2.805	68.9	75.4	8.6

again or the crack propagates to finite life. The experimentally determined crack extensions until crack arrest occurs are drawn as green points in the diagrams. As can be seen from Fig. 10, good agreement between model predictions and experiment is observed. Table 3 compares the experimental and the predicted threshold stress range. As it can be seen, the percentage discrepancy between experiment and prediction is higher the smaller the crack extension length Δa. In general, the experiments showed a slightly lower threshold stress range than the prediction. Therefore, for a damage tolerance assessment of cyclically loaded components, a safety factor in the threshold predictions has to be taken into account and/or the fit of the crack resistance curve (cf. Fig. 4) should be chosen more conservative.

5. Conclusion

Based on a simple mechanical model, a 3-dimensional KT diagram was proposed considering the fact that a crack consists of two different contributions, namely the notch depth where fracture surface contact does not take place and a real crack extension. It was shown that it depends on both contributions – rather than only on their sum – whether a crack is in the area of non-propagating cracks or in the finite life area. Finally, the modified KT diagram was verified using experimental data. Special attention has to be paid to the fact that the deeper the initial notch is compared to the total crack length, the lower is the resistance against crack propagation. If one does not consider this marked influence of the initial notch depth, the endurance limit of a component may be severely over-estimated. In this respect, the modified KT diagram is expected to become a useful tool for the damage tolerance assessment of notched components.

Finally, especially for possible applications in mechanical design and damage tolerance assessment, one has to keep in mind the scope of validity of the proposed model with respect to crack length, loading and notch geometry:

The derivation has been based on Mode I stress intensity factor for physically short cracks. Description of crack closure and loading by the cyclic crack resistance curve and Mode I stress intensity factors does not allow for a description of the behaviour of microstructurally short cracks; this means that the initial crack length has to exceed the largest characteristical microstructural length scale. Cracks of this size typically grow in Mode I perpendicular to the direction of the maximum principal stress; i.e., it has been implicitly assumed here that the maximum principal stress is perpendicular to the crack flanks. Although the examples were given for alternating loading (load ratio $R = -1$), the KT diagram can be constructed easily for any load ratio R: one needs only the appropriate crack resistance curve measured at that specific R value as well as the fatigue endurance limit; the latter can be obtained from high cycle fatigue testing at that R value, or – if at hand – from the Haigh diagram of the material. As the build-up of crack closure is modelled by means of the cyclic crack resistance curve, crack closure at any time depends only on the current crack extension Δa and not on the loading history; i.e., as it is typical for the standard LEFM approach, overload effects and load history effects other than the dependence of the stress intensity factor on the current stress and crack length are not accounted for.

Concerning the geometry of the notch, it is modelled as a sharp crack of length a_0, thereby giving an upper bound for notches of any acuity. For blunt notches, the diagram will therefore give conservative predictions. If the geometry of the initial notch is known exactly, more precise estimates may be obtained by using appropriate geometry factors [12,13]. The modelling concept becomes then formally equivalent to the fictitious crack method [14] except that it assesses the behaviour of actually observed cracks; vice versa, the length of the observed non-propagating cracks could be useful for predicting the averaging length for the fictitious crack model.

Acknowledgements

Financial support by the Austrian Federal Government (in particular from Bundesministerium für Verkehr, Innovation und Technologie and Bundesministerium für Wirtschaft, Familie und Jugend) represented by Österreichische Forschungsförderungsgesellschaft mbH and the Styrian and the Tyrolean Provincial Government, represented by Steirische Wirtschaftsförderungsgesellschaft mbH and Standortagentur Tirol, within the framework of the COMET Funding Programme is gratefully acknowledged.

References

[1] Kitagawa H, Takahashi S. Applicability of fracture mechanics to very small cracks or cracks in the early stage. In: Proceeding of the second international conference on mechanical behavior of materials. ASM; 1976. p. 627–31.
[2] El Haddad MH, Topper TH, Smith KN. Prediction of non-propagating cracks. Eng Fract Mech 1979;11:573–84.
[3] Pippan R, Berger M, Stüwe HP. The influence of crack length on fatigue crack growth in deep sharp notches. Metall Trans 1987;18A:429–35.
[4] Tanaka K, Akiniwa Y. Resistance-curve method for predicting propagation threshold of short fatigue crack at notches. Eng Fract Mech 1988;30(6):863–76.
[5] Suresh S, Ritchie RO. Propagation of short fatigue cracks. Int Met Rev 1984;29(6).
[6] Richtie RO. Mechanisms of fatigue crack propagation in metals, ceramics and composites: the role of crack tip shielding. Mater Sci Eng 1988;103:15–88.
[7] Newman JC, Phillips EP, Swain MH. Fatigue-life prediction methodology using small-crack theory. Int J Fatigue 1999;21(2):109–19.
[8] McEvily AJ, Minakawa K. On crack closure and the notch size effect in fatigue. Eng Fract Mech 1987;28:519–27.
[9] Chapetti MD. Fatigue propagation of short cracks under constant amplitude loading. Int J Fatigue 2003;25(12):1319–26.

[10] Tabernig B, Powell P, Pippan R. Resistance curves for the threshold of fatigue crack propagation in particle reinforced aluminium alloys. In: Newman Jr JC, Piascik RS, editors. Fatigue crack growth thresholds, endurance limits, and designs, ASTM STP 1372. West Conshohocken (PA): American Society for Testing and Materials; 2000. p. 96–108.
[11] Maierhofer J, Pippan R, Gänser HP. Modified NASGRO equation for physically short cracks. Int J Fatigue 2014;59:200–7.
[12] Lukáš P. Stress intensity factor for small notch-emanated cracks. Eng Fract Mech 1987;26:471–3.
[13] Schijve J. The stress intensity factor of small cracks at notches. Fatigue Fract Eng Mater Struct 1982;5(1):77–90.
[14] Taylor D. Geometrical effects in fatigue: a unifying theoretical model. Int J Fatigue 1999;21:413–20.